

MSSW TRANSVERSAL FILTERS BASED ON CURRENT WEIGHTING IN NARROW (10 μ m) TRANSDUCERS

Y.J. Ataiiyan, J.M. Owens, K.W. Reed, R.L. Carter, W.A Davis

The Center for Advanced Electron Devices and Systems (CAEDS)
The University of Texas at Arlington, Arlington, Tx. 76019

ABSTRACT

A Magnetostatic Surface Wave, tunable bandpass filter using current weighted transducer arrays based on transversal filtering techniques has been built. A 100 MHz bandpass filter was realized with a minimum insertion loss of 15 dB and sidelobe suppression of 20 dB. The usable tunability range of the device was from 2 to 3.5 GHz.

INTRODUCTION

Magnetostatic Wave (MSW) devices have opened a new door to high frequency signal processing above 1 GHz, where Surface Acoustic Wave (SAW) devices have high insertion loss and are difficult to fabricate. One area that has eluded researchers has been the development of tunable MSW transversal filters. This paper presents results on the realization of the first synthesized MSW transversal filters. Progress in this area has been slow, primarily as a result of the dispersive nature of MSW's, strong coupling of radiating current elements, interaction between neighboring elements, and reflections from the elements in the array. To overcome the first problem, a computer program was developed to synthesize the desired bandpass filter. This was based on theoretically calculated insertion loss and frequency data for a zero-path length delay line with single bar transducers on both the input and the output. The program generated the normalized current distribution for each transducer element. A bandpass filter utilizing nondispersive waves (e.g. SAW), would require a current distribution of the form $\text{SIN}(X)/X$. Conversely, for MSW's the current distribution must be distorted to compensate for the dispersion of the wave. In order to reduce element interaction and reflections from the array, transducer elements were made as narrow as possible (10 μ m for operation with a 300 μ m center-band wavelength), and in order to limit coupling short open circuited transducers

were used.

THEORY

Magnetostatic Waves (MSW) are basically magnetically coupled dispersive waves that propagate in a magnetically biased ferrite material such as Yttrium Iron Garnet (YIG). The theoretical and experimental characteristics of the MSW technology are well documented elsewhere [1,2,3,4].

Regardless of the type of the wave in the propagating medium (SAW or MSW) and independent of the weighting technique, the procedure for synthesizing a filter is fundamentally the same [5,6]. For a non-interacting N element transducer array with a weighting factor of a_n for each element and path-length ℓ_n , the array response can be written in the form:

$$\tilde{G}(\omega) = \sum_{n=1}^N a_n \tilde{A}(\omega) e^{-K(\omega) \ell_n} = \sum_{n=1}^N \tilde{\Psi}_n(\omega) \quad (1)$$

where,

 $\tilde{G}(\omega)$ = array response $\tilde{A}(\omega) = \alpha + j\beta$ (α and β are loss factor and wave number, respectively) $\tilde{\Psi}_n(\omega)$ = n th element response.

The quantity $\tilde{A}(\omega)$ denotes the complex value of the transmission response for a single-bar/single-bar transducer pair with zero path. This transducer characteristic is obtained by modeling the transducer filaments as a simple lossless microstrip in a manner described by Wu [7]. A pointing vector calculation is used to define a radiation resistance representative of the coupling to the ferrite.

The linearized array response given in equation (1) can be made to fit the desired frequency response of the array,

$\tilde{H}(\omega)$. The R.M.S error, ϵ , can be calculated from equation (2).

$$\epsilon = \frac{1}{\omega_2 - \omega_1} \int_{\omega_1}^{\omega_2} \left\{ \tilde{H}(\omega) - \sum_{n=1}^N \tilde{a}_n \tilde{A}(\omega) e^{-\tilde{K}(\omega) \ell_n} \right\}$$

$$x \left\{ \tilde{H}^*(\omega) - \sum_{n=1}^N \tilde{a}_n \tilde{A}^*(\omega) e^{-\tilde{K}^*(\omega) \ell_n} \right\} d\omega \quad (2)$$

which should be minimized with respect to the weighting factors a_m :

$$\begin{aligned} \frac{\partial \epsilon}{\partial a_m} &= \frac{1}{\omega_2 - \omega_1} \left[\int_{\omega_1}^{\omega_2} \tilde{A}(\omega) e^{-\tilde{K}(\omega) \ell_m} \right. \\ &\quad \left. x \left\{ \tilde{H}^*(\omega) - \sum_{n=1}^N \tilde{a}_n \tilde{A}^*(\omega) e^{-\tilde{K}^*(\omega) \ell_m} \right\} d\omega \right. \\ &\quad \left. + \int_{\omega_1}^{\omega_2} \tilde{A}^*(\omega) e^{-\tilde{K}^*(\omega) \ell_m} \right. \\ &\quad \left. x \left\{ \tilde{H}(\omega) - \sum_{n=1}^N \tilde{a}_n \tilde{A}(\omega) e^{-\tilde{K}(\omega) \ell_n} \right\} d\omega \right] \quad (3) \end{aligned}$$

The integrals in equation (3) are conjugate of each other, so the sum can be expressed as twice the real part. Some manipulation yields,

$$\begin{aligned} \frac{\partial \epsilon}{\partial a_m} &= \frac{-2}{\omega_2 - \omega_1} \left\{ \operatorname{Re} \int_{\omega_1}^{\omega_2} \tilde{A}(\omega) \tilde{H}(\omega) e^{-\tilde{K}^*(\omega) \ell_m} d\omega \right. \\ &\quad \left. - \operatorname{Re} \sum_{n=1}^N \tilde{a}_n \int_{\omega_1}^{\omega_2} |\tilde{A}(\omega)|^2 \right. \\ &\quad \left. - [\tilde{K}^*(\omega) \ell_m + \tilde{K}(\omega) \ell_n] \right\} d\omega = 0 \quad (4) \end{aligned}$$

Setting the partial derivatives of the error function with respect to each of the N parameters to zero yields a matrix of N linear, linearly independent equations. For simplicity, parameters M_{ij} and Q_i are defined as:

$$M_{ij} = \operatorname{Real} \int_{\omega_1}^{\omega_2} |\tilde{A}(\omega)|^2 e^{-[\tilde{K}^*(\omega) \ell_i + \tilde{K}(\omega) \ell_j]} d\omega$$

$$Q_i = \operatorname{Real} \int_{\omega_1}^{\omega_2} \tilde{A}^*(\omega) \tilde{H}(\omega) e^{-\tilde{K}^*(\omega) \ell_i} d\omega$$

The set of equations in (4) can be expressed as,

$$\begin{vmatrix} M_{11} & M_{12} & M_{13} & \dots & M_{1N} \\ M_{21} & \cdot & \cdot & \dots & \cdot \\ \cdot & \cdot & \cdot & \dots & \cdot \\ M_1 & \cdot & \cdot & \dots & M_{NN} \end{vmatrix} \times \begin{vmatrix} a_1 \\ a_2 \\ \cdot \\ \cdot \\ a_N \end{vmatrix} = \begin{vmatrix} Q_1 \\ Q_2 \\ \cdot \\ \cdot \\ Q_N \end{vmatrix}$$

This set of equations can be algebraically inverted to obtain the unnormalized element weighting coefficients, once the numerical integration has been carried out on the matrix elements. The weighting coefficients were then constrained to be real and normalized to unity (-1 to +1).

EXPERIMENTAL PROCEDURE

The 16 element filter in this experiment was designed to have a passband of 100 MHz at the center frequency, $f = 2.7$ GHz, and as much sidelobe suppression as theoretically possible using a 25 μm thick YIG film. The current is distributed among the elements via a simplified 16 way power-divider, which provide phase equalization for each open circuited finger. Individual

transducers within the array are all 10 μm wide and 4mm long, with only 3mm under the YIG (see figure 1). Transducers are fed from both ends with the current weighting in each transducer determined by the placement of an open circuited gap, positioned relative to the longitudinal array axis. As an example, a gap at the center of a transducer would result in a zero net current contribution for that element. It was assumed that in the case of an open-circuited microstrip of length $\ell \ll \lambda/4$, with fringe effects neglected, the current exhibits linear variation along the length. Therefore, the gap in each element was positioned so that the average current on opposing elements had the required sign and value dictated by the synthesis program. In order to reduce the harmonic responses of the array, a shorted $\lambda/2$ spaced loop transducer is used on the output.

The transducers are fabricated from up-plated gold on 10 mil thick, 1" x 1" alumina substrates. The 3mm wide, 25 μm thick YIG film is angle-lapped at the ends to minimize reflections there.

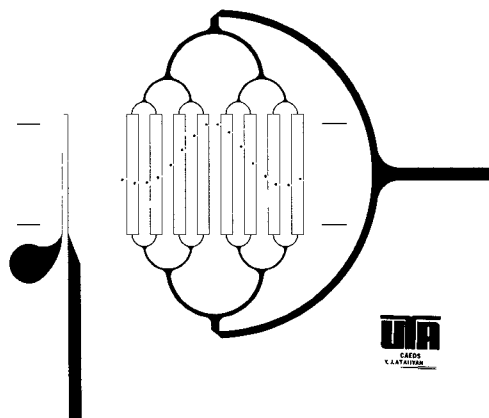


Figure 1: Circuit pattern of the 100 MHz tunable bandpass filter. The position of the gap is marked with "•" at the left side for each transducer. Actual dimension: 1" x 1".

EXPERIMENTAL RESULTS

Figure 2 shows the theoretical prediction of the insertion loss versus frequency for a typical filter with the desired characteristics described earlier. The minimum insertion loss of the fabricated device was observed to be -25dB, which is mainly due to the power-divider mismatch and associated 20:1 VSWR in the passband of the filter. Figure 3 is the transmission response for the device in the frequency range of 1.5 GHz to 3.0 GHz. In this picture the output of the device is amplified to show the sidelobe suppression, otherwise not clearly distinguishable from direct breakthrough.

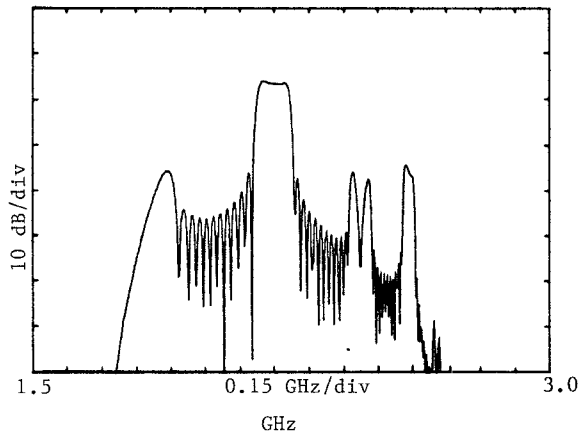


Figure 2: Theoretical prediction of S_{12} .

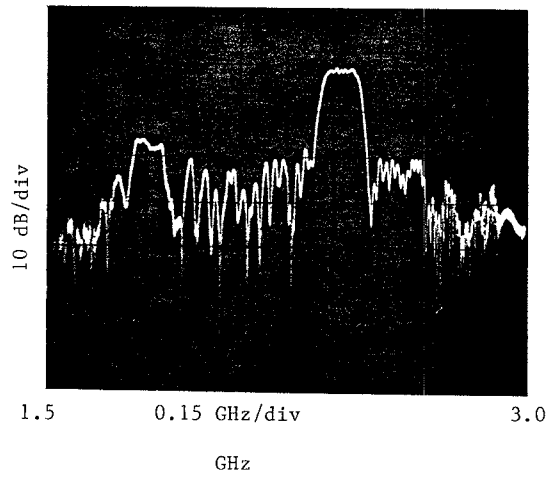


Figure 3: The experimental S_{12} of the device.

The theoretical simulation of the tunability of the filter is shown in figure 4. This was done by superimposing the calculated transmission responses of the filter at four different bias fields. Figure 5 shows the experimental results obtained by varying the magnetic bias field. Figures 4 and 5 clearly demonstrate a decrease in the passband for higher center frequencies. This is due to the band limiting characteristics of MSSW delay line dictated by the applied bias field.

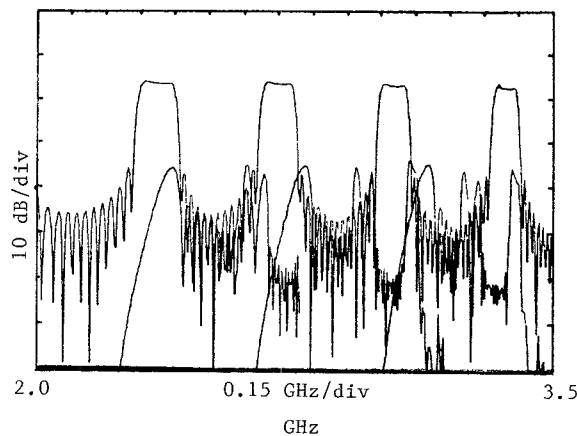


Figure 4: Theoretical prediction for tunability of S_{12} .

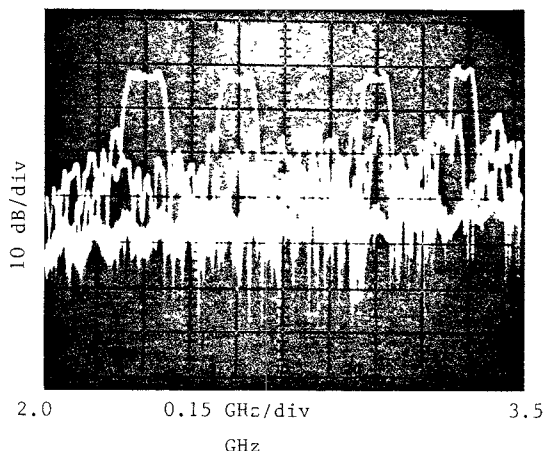


Figure 5: Tunability of S_{12} (200 - 450 Oe).

CONCLUSION

The current weighting technique using open gap transducers to realize MSSW filters, demonstrates a good correlation between the theoretical predictions and obtained performance. With this technique, it is possible to construct a tunable bandpass filter with sidelobe suppression as high as 20 dB, with less than 3 dB amplitude ripple. The variation of the minimum insertion loss in the tunable range of the device can be as low as 2 dB. An improvement of about 10 dB on the minimum insertion loss was achieved by a narrow band matching of the existing power-divider. Therefore, we believe further improvement in delivering the maximum power to each finger via construction of a better matched broad band power-divider can bring the minimum insertion loss close to -10 dB.

ACKNOWLEDGMENT

The authors wish to acknowledge the support of the Army Research Office (ARO) under grant No. DAAG2982K0073 and Rome Air Development Center (RADC) under grant No. F19628-84-K-0029.

REFERENCES

- [1] J.M. Owens and C.V. Smith Jr., "Beyond SAW Filters: Magnetostatics Show Promise", MSN, P.44, June 1979.
- [2] M.R. Stiglitz and J.C. Sathares, "Magnetostatic Eaves Take Over Where SAWs Leave Off", Microwave Journal, P.18, February 1982.
- [3] J.M. Owens and R.L. Carter, "Magnetostatics Advance: The Shape of Waves to Come", MSN, P.103, March 1983.
- [4] H.L. Glass and M.T. Elliot, paper 08.3-8, 10th International Conference Crystallography, Amsterdam, August 1975.
- [5] D.S. Humphreys, "The Analysis, Design, and Synthesis of Electrical Filters", Prentice-Hall, Inc., N.J., Chapter 6, 1970.
- [6] K.W. Reed, "Magnetostatic Ion Implanted Reflective Array Filters", Dissertation, Univ Texas Arlington, Dec. 1985.
- [7] H.J. Wu, "Magnetostatic Wave Transducers", Dissertation, Univ Texas Arlington, Dec. 1978.